Christopher J. Berthelette, Germano S. Iannacchione, Stephan Koehler, and Marko B. Popovic

The One-To-Many Concept and Soft Robotics ExoMusculature

***Abstract*— This paper presents a unique and innovative approach for Soft-Robotics that introduces the "One-to-Many" design concept. This concept allows a single artificial actuator to store energy in the form of potential energy and drive multiple degrees of freedom. Utilized in an ExoMusculature, this approach has many advantages over existing technologies for assistive and augmentative applications. The basic elements have been designed and prototyped along with physical simulations. A biologically inspired control system has been developed and the results of the simulation were compared with the results of a human arm neuro-motor control experiment. Performance improves dramatically with increased numbers of artificial muscle motor units.**

I. Introduction

The force produced by muscles can be modulated by controlling the number of fibers that are activated in parallel, a process known as recruitment. This modulation of force enables optimized efficiency over a wide range of loads and contraction velocities as well as accelerations [1-3]. For the human body, there are about 400 skeletal muscles, each of which is composed of one hundred or more individual motor units. For example, biceps brachii have about 750-800 such motor units [4-5]. Each motor unit represents a single independently actuated degree of freedom (DoF). Hence, if an artificial assistive exo-musculature is to mimic just one percent of human musculature, the number of actuated DoF has to be on the order of one hundred to one thousand. However, conventional approaches involving one dedicated electric motor per actuated DoF result in systems that are very large, heavy, and expensive. This is clearly inappropriate for a fully mobile, wearable exo-musculature.

Here, we propose to resolve this problem by a "One-To-Many" (OTM) concept that allows a single artificial actuator (an electric motor for example) to store energy in the form of elastic potential energy and drive multiple actuated DoF. Critical for this concept are the OTM architecture (Section 2) and a low-power, light weight, high-speed, energy efficient, robust clutch that provides position sensing (Section 3). Our design can be easily miniaturized for more advanced applications. In essence, these clutches are the mechanical analogue of valves for pneumatic and hydraulic systems.

An advantage of a pneumatic actuation system is that a single tank of compressed air can distribute mechanical energy via a network of tubes, valves and pistons, for many independently actuated DoF. These systems can be used effectively as pneumatic muscles for lower [6] and upper [7] extremities, though with limited mobility. For fully mobile, wearable applications, the low energy density of compressed air results in impractically heavy pneumatic systems.

For example, a 180 lb (82 kg) average human walking at 4.00 mph (6.44 km/h) burns approximately 384 nutritional calories (1.61 MJ) per hour [8]. Practical achievable energy density at the motor shaft for a pneumatic system is about 40-100 kJ/kg. Hence, the mass of the compressed air system required for one hour of walking using a whole body exoskeleton system with same cost of transport as human is 28-145 kg. This translates to at least 6-20 standard 5-liter compressed air bottles per hour. A lithium battery has an energy density of 1.3 MJ/kg and its required mass is only 1.24 kg per hour.

Typically, actuators ("muscles") are brought together as a system attached to some rigid frame ("skeleton"). For assistive or augmentative systems, this rigid frame may be in the form of an orthotic or exoskeleton system consisting of rigid links and joints for the lower [9] and upper body [10] extremities. Similarly, most previous actuated systems for upper body rehabilitation use rigid exoskeletons or rigid link manipulators [11-12]. However, this traditional approach has limited DoF and reduced comfort for the user. Due to substantial skin-bone relative motion, misalignments between biological and artificial joints are inevitable. Likewise, misalignments occur when putting on and taking off the exoskeleton. These complications in all cases make exoskeletons with rigid joints uncomfortable. Furthermore, misalignments, especially for the lower extremities, can lead to lesions and bone fractures due to the large forces they are subject to.

Figure 1.Soft Robotics ExoMusculature : wearable, compliant, light-weight, cost-effective, adaptive artificial muscle network for rehabilitation, augmentation, 3D Internet or tele-operation with haptic/force feedback [13-15, 18]. Here, the shoulder brace, on the right, attached to a mannequin arm with added weights is tele-operated by the human arm movements [15,18]

Manuscript received March 10, 2012.

C. J. Berthelette (c.berthelette@wpi.edu) , G. S. Iannacchione (gsiannac@wpi.edu) , S. Koehler (sak@wpi.edu) , and M. B. Popovic (mpopovic@wpi.edu) are with Worcester Polytechnic Institute, 100 Institute Rd., Olin Hall, Worcester, MA 01609-2280, USA.

These problems are resolved in our approach as the Soft Robotics ExoMusculature is a *compliant*, thin, light-weight, self-actuated multi-component garment without singular joints or rigid elements [13-15]. Other soft robotic pneumatic [6-7] or cable driven devices [16-17], also take advantage of natural anatomical structures, including joints and bones, to provide the device structure and maintain the natural kinematic DoF. Additionally, the adaptive control identifies linear and angular misalignment parameters of the exomusculature relative to the wearer and self-compensates for optimal actuation [18].

In Section 4 we introduce the detailed OTM physical model, describe the biologically inspired control system, and present results of simulation tests. In Section 5, we report on a human arm neuro-motor control experiment and compare biological and artificial system results.

II. One-To-Many Concept System Design

The simplified schematic of the OTM concept is shown in Fig 2. The OTM design provides a mechanism for storing and distributing mechanical energy from a single motor to many independent motor units (actuated DoFs). This is an electromechanical analogue of a pneumatic or hydraulic system.

The central motor is coupled to the individual motor units via a system of cables and clutches. The clutch mechanisms actuate only a small blocking mass that catches a cable with minimal energy losses due to friction. The clutches allow a single high power central motor to store elastic energy in each motor unit in a short period of time. This energy can then be released at any time via another “down-stream” clutching mechanism to actuate a cable (DoF) in a finely controlled manner.

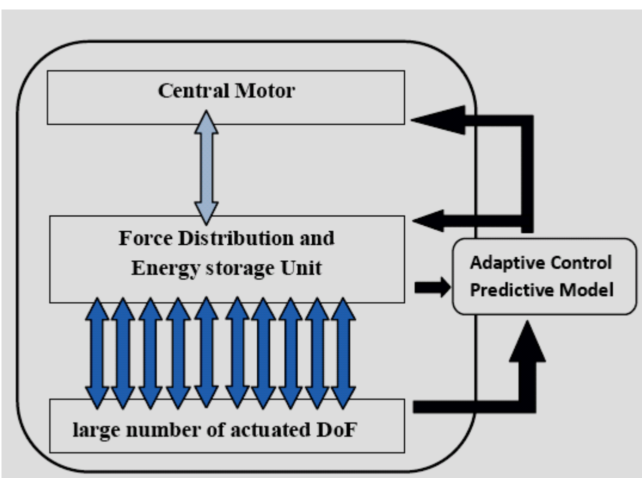

Figure 2. Schematic of the OTM concept.

III. Clutch Mechanisms

Mechanical clutches allow the manipulation of power transmission and can be sorted into two distinct types: positive clutches and friction clutches. A positive clutch is a device with two mating surfaces that directly engage each other with interconnecting elements that prevent slipping during the transmission of power. A friction clutch utilizes friction force to engage the mating surfaces in the device. An example of a positive clutch applicable to the OTM concept is demonstrated in a Transtibial prosthesis that is comprised of cams with teeth that interface with a threaded bar [19]. Examples of friction-based devices researched when designing the OTM clutch mechanism include Cam Cleat devices and Jam Cleat devices [20].

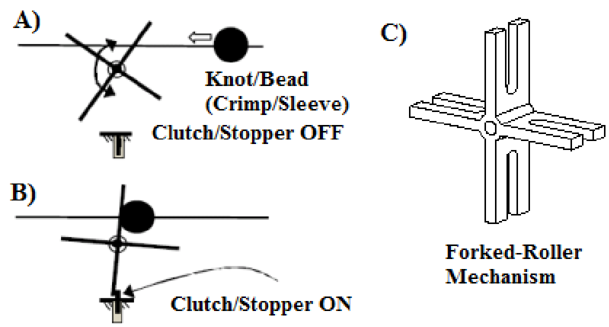

Figure 3 Clutch utilizing forked-roller mechanism with small stopper

The most critical element in the OTM system is the OTM clutching mechanism. One of the possible design solutions is shown in Fig 3. Taking into account small travel distances (<2 mm) and low friction (<0.1), the clutch will require less than 0.02J of energy for a 100N cable force to transition from the ON state to OFF state. Here, the active force is perpendicular to the cable tension. Hence, the tension is counteracted by the mechanism’s passive force. In Fig 3, the forked roller is engaging with small beads fixed at equidistant positions along the length of the cable. High bead density and clutch bandwidth will support fine control of energy released by the elastic elements in the device.

The OTM system requires the designed clutch mechanism to be a high frequency, low power, cost-effective device that can withhold very large forces and that can be easily miniaturized. Therefore, the following design criteria were prioritized: (a) a small travel distance by active mobile part, (b) force primarily blocked by passive immobile structure (c) minimal friction losses between active mobile part and the rest of the system.

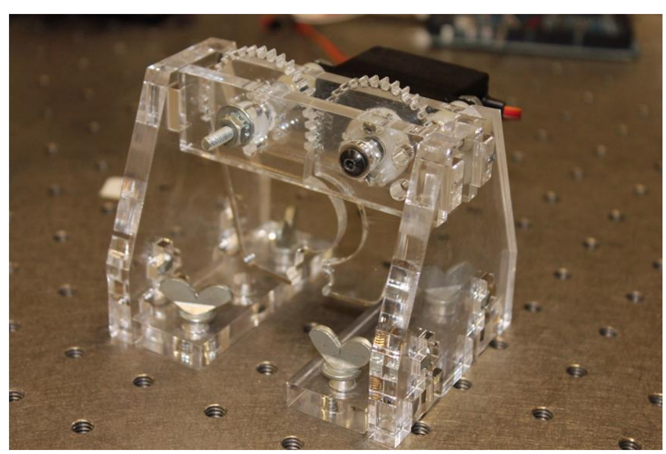
Figure 4 Clutch utilizing Claw/Gear Mechanism

Based on these system requirements, two positive macro-scale clutches have been developed for the OTM concept application. The first utilizes a claw mechanism incorporating gears and a servo motor to open and close the device to engage the cable, see Fig 4.

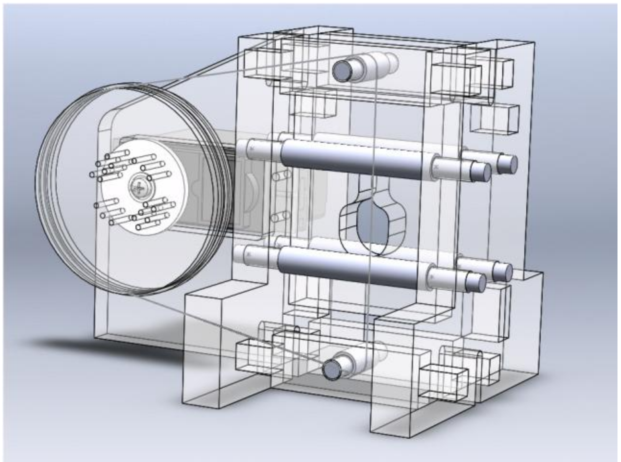

Figure 5 Clutch utilizing sliding-gate mechanism

The second clutch developed utilizes a sliding-gate which moves vertically controlling the width of a slot on the plate itself. The second clutch provides a structure allowing the plate to move with minimal losses due to friction force. The width of the slot will either allow the cable to pass through the clutch with zero contact or will engage the cable, Fig 5.

Several other hybrid mechanisms i.e. cross between hydraulic, pneumatic, and electromechanical methods are currently being examined.

IV. Physical Model and State Machine Simulation

A. Physical Model

A closed loop conveyor system was created to drive the system comprising of a cylindrical drive roller R1 (directly connected to the main motor), and a cylindrical return roller R2. The cables connecting R1 and R2 have aluminum stop sleeves (cable crimps) spaced equidistant on each closed loop to provide many points of contact on each cable for the clutches to engage. R1 and R2 operate independently from the rest of the system. The number of motor cables connecting R1 and R2 equals to the number of independently actuated motor units.

The OTM system may consist of many motor units. Each of these subsystems, see Fig 6 is envisioned to have 3 clutches (C1, C2, C3), 2 elastic elements (E1, E2), 2 cables (motor cable, "muscle" fiber) with aluminum stop sleeves (cable crimps) spaced at equidistant points along the cables, and an additional roller (R3) per "muscle" fiber.

The clutches have two conditions. The first condition, *Open*, allows the cable with stop sleeves (cable crimps) to pass freely through the clutch with zero contact. The second condition, *Closed*, allows the cable to pass with minimal interference but directly engages with a stop sleeve (cable crimp) to create the clutching effect on the motor cable or on the "muscle" fiber motor unit cable.

The C1 clutch can move linearly along the cable path and it may engage with both the “muscle” motor unit cable and the motor cable (i.e. one of the cables connecting rollers). The C2 and C3 clutches have a fixed position and they may only engage with the “muscle” fiber motor unit cable.

The elastic roller R3 takes fiber slack but does not generate forces that substantially affect load dynamics.

The E1 elastic element (spring constant k1) stores motor energy that is then distributed at a later time to the E2 elastic element (spring constant k2) and load itself (mass M).

The motor unit subsystem proceeds trough 4 consecutive phases:

- Phase 0 (C1 open, C2 open, C3 open): R3 regulates fiber length and E1, E2 in equilibrium.
- Phase 1 (C1 closed, C2 open, C3 closed): Motor energy transferred to elastic element E1.
- Phase 2 (C1 open, C2 closed, C3 closed): Energy stored in elastic element E1.
- Phase 3 (C1 open, C2 closed, C3 open): Energy transferred to elastic element E2 and load.

B. Control Algorithm

The control mechanism for two antagonistic muscles, see Fig 7, is simplified to case of the state machine where one single motor unit is actuated at a time. The actuated motor unit transitions through four phases (0, 1, 2 and 3) while the non-actuated motor unit stays in phase 0.

At the end of the actuation cycle the actuated motor unit resets to phase 0 during which the springs quickly return to their equilibrium values while load state (position and velocity) stays unchanged. The duration of each phase

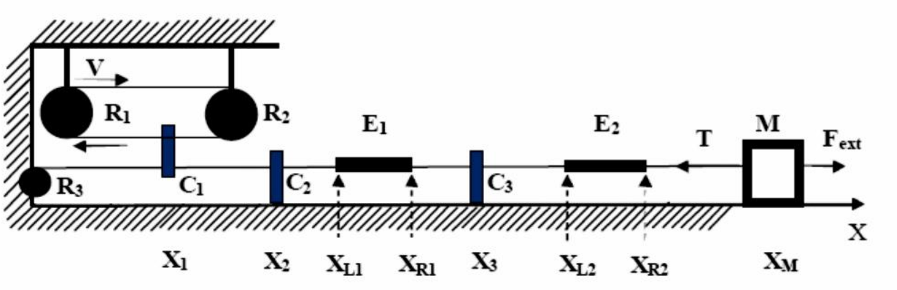

Figure 6 The single motor unit consists of 3 clutches (C1, C2, C3), 2 elastic elements (E1, E2) and roller R3 that takes a “muscle” fiber slack. Also shown are rollers R1 and R2 that are shared by many motor units from same or different “muscles”.

transition is δt.

The R1 and R2 rollers (driven directly by the main motor) are assumed to provide a linear constant speed V.

The actuated fiber is selected at beginning of phase 1 based on predicted value of

$$\Delta_{pred}\theta_T = (\theta_T - \theta)_{pred} \quad (1)$$

at time $t_3 = t_1 + \delta_1 t + 2\delta t$ (i.e. beginning of phase 3). For positive (negative) values, the back (front) motor unit is actuated. Here, we assume that 2^{nd} phase has zero duration. In the case of multiple motor units per muscle, this interval may not be zero.

The duration of the 1^{st} phase can be defined by the control requirement that motor-added energy is equal to difference of energy that the arm would have if it has the target predicted state at control time $t_1 + 3\delta t$ and actual arm energy at time t_1 (i.e. beginning of phase1)

$$\frac{1}{2}k_1V^2(\delta_1 t)^2 = \frac{1}{2}I\left(\omega_{Tpred}^2 - \omega^2\right) + \frac{1}{2}k_2R^2\left(\theta_{Tpred} - \theta\right)^2 \quad (2)$$

with $\omega_{Tpred} = \omega_T + \alpha_T(3\delta t)$ and $\theta_{Tpred} = \theta_T + \omega_T(3\delta t) + \frac{1}{2}\alpha_T(3\delta t)^2$ at control time $t_1 + 3\delta t$ and $\theta_T, \omega_T, \alpha_T$ the target values at beginning of phase 1. However, since the right hand side is not positive definite, we instead utilized the modified co-rotating frame energy

$$\frac{1}{2}k_1V^2(\delta_1 t)^2 = \frac{1}{2}I\left(\omega_{Tpred} - \omega\right)^2 + \frac{1}{2}k_2R^2\left(\theta_{Tpred} - \theta\right)^2 \quad (3)$$

The dynamics of the arm from time $t_1$till t_3 are passive dynamics obeying

$$\tau = \left(T_f - T_b\right)R = -k_2R^2\Delta\theta\,\frac{1 \mp sign(\Delta\theta)}{2} = I\alpha \quad (4)$$

whereas dynamics of the arm from time $t_3$till t_0 is passive dynamics obeying

$$\tau = \left(T_f - T_b\right)R = \frac{k_1k_2R}{k_1+k_2}\left[(V\delta_1 t - R\Delta\theta)\delta_f^\gamma - (V\delta_1 t + R\Delta\theta)\delta_b^\gamma\right] = -\frac{k_1k_2R}{k_1+k_2}(R\Delta\theta \mp V\delta_1 t) = I\alpha \quad (5)$$

with $\Delta\theta = \theta - \theta_{equ}$ and minus (plus) sign for the actuated front (back) motor unit.

Phase 3 continues while function $|\theta - \theta_T + c\omega{-}\omega T\delta t$ decreases. Finally, the parameter c is chosen to best address the actual system dynamics.

Adding more motor units to each muscle and applying the same control algorithm effectively results in summing the spring constants for parallel multi-fiber motor unit systems.

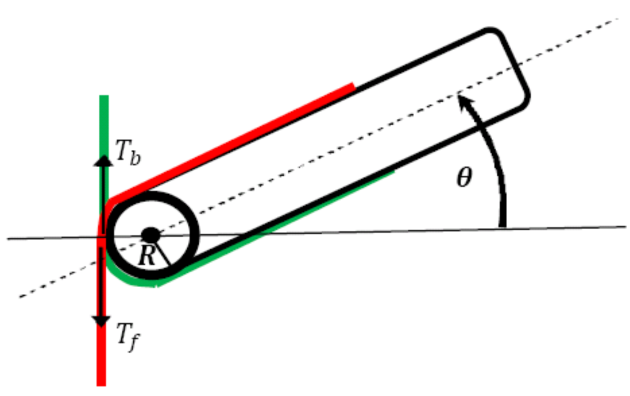

Figure 7. Simple Arm Model: pair of antagonistic muscles.

C. Simulation Result

The first simulation experiment was performed with static target at -60°, see Fig 8. The arm's initial conditions at time 0 were set to 0° and zero angular speed.

The arm was moved by antagonistic muscles consisting of 1,2,4,8, and 12 fiber motor units. Each fiber motor unit spring constant was set to 5kN/m. The constant ***c*** was set to 45. The phase transition duration was set to 10 ms.

As expected, the system performance in terms of position control dramatically improves when multiple motor units are added in parallel. A muscle with a single motor unit undershoots the predetermined target by almost 15^0 degrees and it stabilizes within a $60^o \pm 1^o$ interval in about 3 sec. A muscle with 12 motor units undershoots the predetermined target by less than 5^0 degrees and stabilizes within a $60^o \pm 1^o$ interval in about 1 sec.

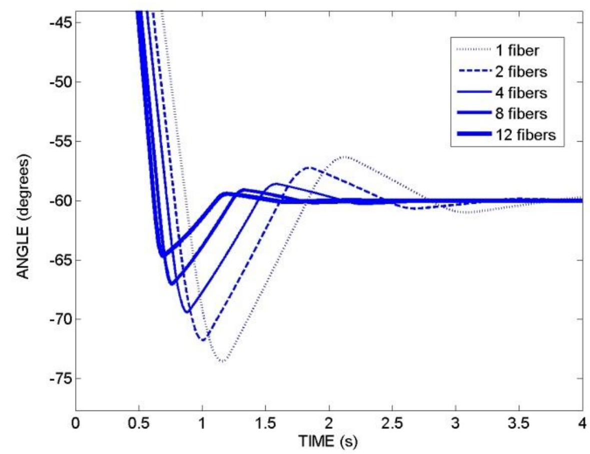

Figure 8 The static experiment: Arm trajectory with varied number of recruited muscle motor units.

V. Human Subject Experiment

A. Methods

Two healthy adult male experimental subjects, MP and IG, performed 4 ~20sec trials each in an experiment where they were instructed to keep their torso static, and to try to align their arm (kept in straight posture) with a moving target. "Aligned", here, means that arm axis coincided with shoulder-target axis. The target was randomly moved by a researcher. The distance from the experimental subject's shoulder was kept approximately constant at about 10 cm from the arm end-effector (fist) if the arm was ideally aligned. The subject MP performed the first trial, had a 1 min break, then performed 3 connected trials without a break. The subject IG performed 4 connected trials. The position and relative orientation of the trunk, shoulder, arm and target were obtained with *Flock of Birds* EM trackers and the relative angle between the arm axis and shoulder-target axis as well as shoulder-target axis angular speed were calculated [15].

B. Experimental Results

The arm *effective response time*, Fig.9, is defined as the ratio of the mean of the erroneous angle, i.e. angle between arm and shoulder-target axes, and the mean of the target angular speed. In the experiment with two subjects, 4 ~20 s trials each, we found:

(1) The effective response time is not smaller than 50 ms and has a very strong tendency to increase over time (it approximately doubles after 1 minute mainly due to fatigue).

(2) The accuracy of the human arm angular displacement (for target average angular speeds per trial in range 60^0-100^0 per second) is not better than 5 degrees (typically on the order of 10 degrees), Fig 10. Moreover, it is uncorrelated with target speed, and has a very strong tendency to increase over time.

C. Comparison of Simulation and Human Arm Experiment

We performed a preliminary simulation control study with predetermined target trajectory identical to the one in the human arm experiment. We observed that simulation trajectory can closely resemble the actual human arm trajectory if the appropriate (time-dependent) number of motor units are recruited [21]. This should not come as a surprise. The proposed OTM ExoMusculature's elastic element E2 resembles a tendon or passive spring (in the Hill Model)[22] whereas the OTM ExoMusculature's elastic element E1 resembles an active element. Finally, the proposed OTM architecture and proposed control algorithm allow for biologically inspired control of both position and stiffness.

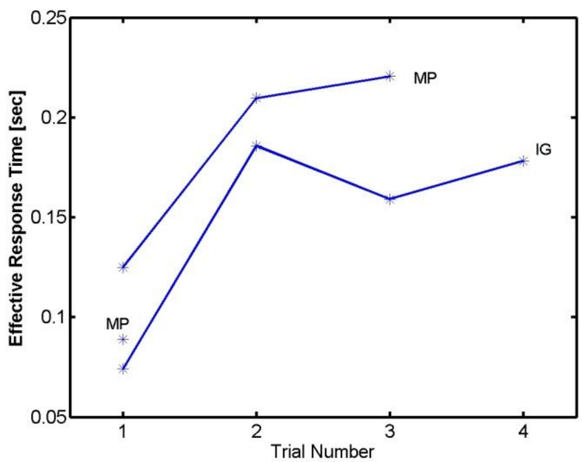

Figure 9. Human Arm following a randomly moving target: Effective Response Time for experimental subjects MP (single trial, short break and 3 connected trials) and IG (4 connected trials).

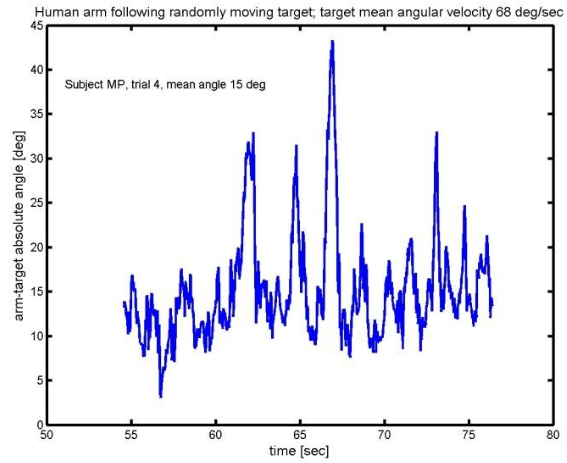

Figure 10. Human Arm following a randomly moving target: absolute angle between arm and shoulder-target axes during third connected ~20sec trial for experimental subjects MP. The shoulder-target axis mean angular speed is 68 deg/sec and mean erronous angle is 15 deg.

VI. Conclusion

We propose the "One-to-Many" design concept that allows a single artificial actuator (e.g. electro-motor) to store energy in the form of elastic potential energy and drive multiple DoFs by utilizing an advanced clutching mechanism. This concept might be quite beneficial for systems like ExoMusculature that, if biologically realistic, necessitate a very large number of actuated DoFs. The practical system can be made very compact, light weight, low power (hence energy efficient) and finally cost-effective. Furthermore, we argue that pneumatic driven ExoMusculatures are inappropriate for the full mobility due to small energy density.

We report on our current work on clutching mechanisms. We present in detail one possible realization of the OTP system with 3 clutches and 2 elastic elements in series per actuated DoF, i.e. ExoMusculature's motor unit. Still further, we propose the biologically inspired control architecture that simultaneously allows for both position and stiffness control via "muscle" recruitment of multiple motor units. Finally, we contrast the simulation results with a human arm experiment.

Our future work will entail continued development of low-power, high bandwidth, robust clutching mechanisms and continued investigation of different control modalities of biologically inspired multiple DoF Exomusculature.

Acknowledgment

M. B. P. thanks the American Institute of Physics for financial support and best SPS project award at the national level in 2011. The authors thank Bo Rim Seo for her contribution regarding the friction based clutches and study of friction effects on currently developed clutches.

References

[1] I. Hunter & S. Lafontaine, "A comparison of muscle with artificial actuators", *Technical Digest IEEE Solid State Sensors & Actuators Workshop*, 1992, pp. 178-185.

[2] R. Full and K. Meijer "Metrics of natural muscle." In *Electro Active Polymers (EAP) as Artificial Muscles, Reality Potential and Challenges*, ed. Y. Bar-Cohen, 67-83. SPIE Press 2001.

[3] John D. Madden, Nathan Vandesteeg, Patrick A. Anquetil, Peter G. Madden, Arash Takshi, Rachel Z. Pytel, Serge R. Lafontaine, Paul A. Wieringa and Ian W. Hunter, "Artificial Muscle Technology: Physical Principles and Naval Prospects", IEEE Journal of Oceanic Engineering, Vol. 29, No. 3, p. 706, July 2004.

[4] Goldspink, G. (1985). Malleability of the motor system: A comparative approach. Journal of Experimental Biology, 115, 375-391.

[5] Guyton, A.C. (1991). Medical Physiology. 8th ed. Philadelphia: W.B. Saunders.

[6] Y.-L. Park, B. Chen, D. Young, L. Stirling, R. J. Wood, E. Goldfield, and R. Nagpal, "Bio-inspired Active Soft Orthotic Device for Ankle Foot Pathologies" in Proc. IEEE/RSJ Int. Conf. Intell. Rob. Syst., San Francisco, CA, September 2011.

[7] J. Ueda, et al. "Individual Muscle Control Using an Exoskeleton Robot for Muscle Function Testing", IEEE Trans. On Neural Sys. And Rehab. Eng., vol, 18, n 4, 2010, pp 339-350.

[8] William D. McArdle, Frank I. Katch, and Victor L. Katch "Exercise Physiology: Nutrition, Energy, and Human Performance", Seventh Edition, Lippincott Williams & Wilkins, Nov 13, 2009.

[9] Dollar, A and Herr. H. "Lower Extremity Exoskeletons and Active Orthoses:Challenges and State-of-the-Art" IEEE Transactions on Robotics (2008) Volume: 24, Issue: 1, Pages: 144-158

[10] Gopura, R.A.R.C.; Kiguchi, K.;and Bandara, D.S.V., "A brief review on upper extremity robotic exoskeleton systems", 6th IEEE International Conference on Industrial and Information Systems (ICIIS), 2011.

[11] H. I. Krebs, N. Hogan, et al., "Overview of clinical trials with MIT-MANUS: a robot-aided neuro-rehabilitation facility", Technology Health Care. vol. 7, 1999, pp. 419-23.

[12] L. E. Kahn, et al., "Robot-assisted reaching exercise promotes arm movement recovery in chronic hemiparetic stroke: a randomized controlled pilot study", J Neuroengineering Rehabil., vol. 3, 2006.

[13] S. B. Kesner, L. Jentoft, F. L. Hammond, R. D. Howe and M. B. Popovic (2011). "Design Considerations for an Active Soft Orthotic System for Shoulder Rehabilitation", 33rd Annual International IEEE EMBS Conference , August 30 - September 02, 2011, Boston, USA.

[14] Blumenau, A., Girardo, D., O., Lin, E., L., Mandala, S., and Popovic, M. B, "Physics applied to post-stroke rehabilitation", AIP SPS award June 2011 interim report. (available online at www.spsnational.org/ programs/awards/2011/ugr2011_Worcester.pdf)

[15] Girardo, D. O., and Popovic, M. B, (2011) "Physics applied to post-stroke rehabilitation; Shoulder Soft Robotics Brace", AIP SPS award December 2011 final report. (available at: http://www.spsnational.org/programs/awards/2011/ugr11_WPI.pdf)

[16] E. A. Brackbill, Y. Mao, S. K. Agrawal, et al., "Dynamics and Control of a 4-dof Wearable Cable-driven Upper Arm Exoskeleton", in proceedings of Int. Conf on Robotics and Automation", 2009.

[17] S. K. Agrawal, et al., "Optimization and Design of a Cable Driven Upper Arm Exoskeleton", in proceedings of Int. Design Eng. Tech Conf. (IDETC/CIE), 2009.

[18] Ignacio Galiana, *Student Member, IEEE*, Frank L. Hammond III, *Member, IEEE*, Robert D. Howe, *Senior Member, IEEE* and Marko B. Popovic, "Wearable Soft-Orthotic Device for Post-Stroke Shoulder Rehabilitation: Identifying Misalignments" Submitted to IEEE IROS 2012. (demo available at http://walltrust.com/ALL/SoftRoboticsSuitWeightLifting.AVI)

[19] K. Endo, E. Swart, and H. Herr, An Artificial Gastrocnemius for a Transtibal Prosthesis, Annual International Conference of the IEEE Engineering in Medicine and Biology Society, 2009. EMBC 2009.

[20] Dan Dickison, Editors of Practical Sailor "Practical Sailor Guide to Sailing Gear: Take the Guesswork Out of Gear Buying" The Lyons Press (2006).

[21] M. B. Popovic "One-To-Many ExoMusculature: Comparison of Biological and Artificial Movements", *in preparation* (2012).

[22] Hill,A.V. (October 1938). "The heat of shortening and dynamics constants of muscles". Proc. R. Soc. Lond. B (London: Royal Society) 126 (843): 136–195